

# Properties of pulsating OH/IR stars revealed from astrometric VLBI observation

Akiharu Nakagawa<sup>1</sup>, Tomoharu Kurayama<sup>2</sup>, Hiroshi Sudou<sup>3</sup> and Gabor Orosz<sup>4</sup>

<sup>1</sup>Graduate School of Science and Engineering, Kagoshima University, 1-21-35 Korimoto, Kagoshima, Kagoshima 890-0065, Japan. email: [nakagawa@sci.kagoshima-u.ac.jp](mailto:nakagawa@sci.kagoshima-u.ac.jp)

<sup>2</sup>Teikyo University of Science, 2-2-1 Senju-Sakuragi, Adachi-ku, Tokyo 120-0045, Japan

<sup>3</sup>Department of General Engineering, National Institute of Technology, Sendai College, Natori Campus, 48 Nodayama, Medeshima-Shiote, Natori-shi, Miyagi 981-1239, Japan

<sup>4</sup>Joint Institute for VLBI ERIC (JIVE), Oude Hoogeveensedijk 4, 7991 PD, Dwingeloo, Netherlands

**Abstract.** We aim to reveal properties of evolution stages in AGB phase; Mira, OH/IR stars, and non-variable OH/IR stars. We presented results of our VLBI observations of four stars; NSV17351, OH39.7+1.5, IRC–30363, and AW Tau. We used the VERA VLBI array to observe 22 GHz H<sub>2</sub>O masers. Parallaxes of the four sources were obtained to be  $0.247 \pm 0.035$  mas ( $4.05 \pm 0.59$  kpc),  $0.54 \pm 0.03$  mas ( $1.85 \pm 0.10$  kpc),  $0.562 \pm 0.201$  mas ( $1.78 \pm 0.73$  kpc), and  $0.449 \pm 0.032$  mas ( $2.23 \pm 0.16$  kpc). Determination of pulsation period of NSV17351 was done for the first time. We revealed the position and kinematics of NSV17351 in our Galaxy and found that NSV17351 is located in an interarm region. A new period-magnitude relationship was indicated in the infrared region. Various other properties based on the distance measurements are also discussed. We have to emphasize that the VLBI astrometry is effective and the only way for parallax measurements of dust obscured OH/IR stars.

**Keywords.** VLBI, Astrometry, Masers, AGB stars, OH/IR stars

## 1. Introduction

### 1.1. Evolution of AGB stars

In the last stage of stellar evolution with initial masses of  $0.8\text{--}10 M_{\odot}$ , they go through a phase called Asymptotic Giant Branch (AGB) stars (Karakas & Lattanzio 2014). That is to say, almost all stars will spend a period of their life as the AGB stars. The AGB stars return various elements into interstellar space by stellar winds. So, they are important objects that contribute to the chemical composition of the universe and Galaxy. They often show thick circumstellar dust shells and long pulsation periods. A closer look at the evolution on the AGB phase reveals more detailed stages of their growth. On the early AGB phase, stars have relatively thin dust layers, so we can observe them in optical and infrared bands. Mira type variables are thought to be at this early phase. However, as they progress, they become faint and unobservable in optical band due to the absorption by circumstellar dust shells. Instead, they become brighter in the infrared band due to re-radiation from the outer dust layer. At this stage, many objects represent OH masers in their outermost layer, therefore they are referred to as OH/IR stars. The OH/IR stars, a sub-class of AGB stars, are thought to be at a late stage of the AGB phase before they evolve to planetary nebulae (te Lintel Hekkert *et al.* 1991).

### 1.2. *AGB stars with various initial mass and detailed evolution in AGB phase*

Stellar properties of the AGB stars such as ages, mass loss rates, and pulsation periods depend on their initial masses. There are sub-classes in the OH/IR stars. Massive OH/IR stars with higher luminosity and longer period are classified as a super AGB phase (Karambelkar *et al.* 2019). The OH/IR stars with intermediate mass ( $>5 M_{\odot}$ ) and large mass loss rates ( $>10^{-4} M_{\odot}/\text{yr}$ ) are classified as extreme-OH/IR stars (Justtanont *et al.* 2015). Thus, there are considered to be several stages in the AGB phase depending on its evolution. Mira type variables are at early stage of the AGB phase. They have relatively thin dust shells and frequently show SiO and H<sub>2</sub>O masers. After the Mira phase, the H<sub>2</sub>O molecules are transported to outer side of the circumstellar envelope and then photodissociated to produce OH maser. Due to an excess of infrared emission from the circumstellar dust shell and the presence of OH maser emission, they will be recognized as the OH/IR stars. Before the post-AGB phase, stellar pulsation gradually diminishes, and they experience a phase called non-variable OH/IR stars (Kamizuka *et al.* 2020). To understand the sequential evolution from early to late AGB phases, studies of the AGB stars with various properties are necessary.

### 1.3. *Pulsation period and mass of AGB stars*

The AGB stars with longer pulsation periods are considered to be more massive than ones with shorter periods. According to Feast (2009), AGB stars with pulsation period of 1000 days are considered to have masses of 3-4  $M_{\odot}$ . Mean density and periods of pulsating stars couple each other (Cox 1980). And masses and periods also couple each other (Takeuti *et al.* 2013). For studies of AGB stars with various masses, we need observations of stars with wide period range. In our previous observations with the VERA from 2003 to 2017, we have conducted many VLBI observations toward dozens of AGB stars. Most of the sources are classified as Mira variables and semiregular (SR) variables, so their pulsation periods are shorter than 400 days. From the studies, we have revealed structures and kinematics of circumstellar matters (e.g. (Nyu *et al.* 2011; Nakagawa *et al.* 2016, 2018; Matsuno *et al.* 2020)). However, there are very few VLBI studies which focusing on OH/IR stars. A wide coverage of their pulsation period is necessary to collect AGB stars on various evolutionary phases and masses. Therefore, after 2017, we have started VLBI observations toward OH/IR stars with longer period range. Scope of our long-term VLBI study is to reveal astrometric and physical properties of OH/IR stars (parallax based distance, proper motion, internal maser motion, luminosity, mass loss rate and so on). We think comparisons of these properties between OH/IR stars and Mira variables can bring clues to understand evolutionary relation. On this report, we mainly present current status and results from astrometric VLBI observations. Preliminary results of parallaxes and proper motions are presented.

### 1.4. *Period-Magnitude relation of AGB stars with wide period range*

Using a distance of a source determined from its parallax, we can estimate absolute magnitude of the source. In Nakagawa *et al.* (2018), we reported a relation between their pulsation periods and K-band absolute magnitude (M<sub>k</sub>) of the Galactic long period variables based on our VLBI observations with VERA. As we have mentioned in the previous section, the period coverage of our previous observations is shorter than  $\sim 400$  days. With our new target sources, we can explore the relation in the longer period range and can extend the relation.

### 1.5. Advantage of VLBI on parallax measurements of AGB and OH/IR stars

Chiavassa *et al.* (2018) used three-dimensional radiative hydrodynamics simulation of convection and explored the impact of the convection-related surface structure in AGB stars on the photometric variability. They extracted parallax errors in Gaia DR2 for SR variables in the solar neighborhood and compared it to the synthetic predictions of photocenter displacements. As a result, they reported that position of the photocenter displays temporal excursion between 0.077 – 0.198 au (5 to 11% of the corresponding stellar radius), depending on the simulation considered. At the distance of 1 kpc, this excursion corresponds to 0.077 – 0.198 mas. Since distances of the VLBI target AGB stars in our study are hundred to a few kpc, size of this excursion can be estimated to be 0.1 – 1 mas. Time variation of the surface degrades accuracy of parallax measurements based on optical image. Gaia measurements can be suffered from this effect.

Mira variables which considered to be at an early stage of the AGB phase are bright in both optical and infrared. Recently, the Gaia Data Release 3 (Gaia DR3; Gaia Collaboration *et al.* (2022))† provided a huge amount of astrometric measurements. Parallax of large number of Mira variables are available in the Gaia database. However, if the central star is surrounded by a thick dust layer, the source become faint and they cannot be observable with Gaia. For example, the OH127.8+0.0 is known as an OH/IR star with high mass loss rate and long pulsation period of 1994 days. The OH127.8+0.0 is very luminous in infrared, but we cannot find the source in Gaia DR3 because it is faint in optical band due to circumstellar extinction by the dust layer. In the astrometric observations of such stars, the VLBI can be a powerful and promising tool.

## 2. Observation

### 2.1. Single dish monitoring of H<sub>2</sub>O and SiO maser

We have been observing H<sub>2</sub>O and SiO maser emissions using the 20 m aperture telescope at VERA Iriki station in order to obtain its spectra and variability. Since the pulsation periods of large number of dusty OH/IR stars are not found in the literature or databases, we have to determine the pulsation period from single dish monitoring by ourselves. Integration time of our single-dish observations are 10 to 40 minutes to reduce noise levels (antenna temperature in K) in each observation to less than 0.05 K. Time intervals between the single-dish observations are not necessarily constant, but are approximately one month interval. The conversion factor from antenna temperature to the flux density is 19.6 Jy K<sup>-1</sup>. A 32 MHz bandwidth data with 1024 spectral channels gives a frequency resolution of 31.25 kHz, which corresponds to a velocity resolution of 0.42 km s<sup>-1</sup> at 22 GHz and 0.21 km s<sup>-1</sup> at 43 GHz. We adopted a signal-to-noise ratio (S/N) of 3 to 5 as a detection criterion in our single-dish observations.

### 2.2. VLBI observations and data reduction

We use the VLBI Exploration of Radio Astrometry (VERA) to observed 22 GHz H<sub>2</sub>O and 43 GHz SiO maser emissions of Mira variables and OH/IR stars. The VERA consists of four 20 m aperture radio telescopes at Mizusawa, Iriki, Ogasawara, and Ishigaki-jima. The longest baseline is 2270 km between Mizusawa and Ishigaki-jima stations. Each antenna of VERA is equipped with a dual-beam system (Kawaguchi *et al.* 2000) with which we can simultaneously observe a target maser source and an extragalactic continuum source within a separation angle between 0.3° and 2.2°. The extragalactic sources are used as position references. Using the dual-beam system, we can calibrate short-term tropospheric fluctuations with the phase-referencing technique (Honma *et al.*

† Gaia Data Release 3; <https://www.cosmos.esa.int/web/gaia/data-release-3>

**Table 1.** Gaia DR3 parallaxes of our VLBI target sources.

Source name (2017–2022) <sup>†</sup>	$\Pi_{\text{DR3}}$ [mas]	Err. [%]	Period [days]	Source name (2023–) <sup>†</sup>	$\Pi_{\text{DR3}}$ [mas]	Err. [%]	Period [days]
NSV 17351	0.088±0.147	166	1122	V697 Her	1.029±0.129	13	497
OH 127.8–0.0	na	na	1994	NSV 23099	0.209±0.102	49	431
NSV 25875	na	na	1535	OH 358.667–0.044	0.207±0.142	69	300
RAFGL 5201	–0.131±0.253	–194	600	OH 358.23+0.11	–0.061±0.190	–313	704
OH 83.4–0.9	0.836±0.556	66	1428	OH 0.66–0.07	na	na	na
OH 141.7+3.5	na	na	1750	IRAS 18039–1903	na	na	na
CU Cep	0.231±0.057	25	700	OH 9.097–0.392	0.261±0.232	89	634
RAFGL 2445	–1.548±0.369	–24	na	RAFGL 1686	1.053±0.359	34	500
OH 39.7+1.5	na	na	1260	IRAS 18176–1848	2.404±0.618	26	na
OH 26.5+0.6	na	na	1589	OH 44.8–2.3	0.918±0.631	69	na
OH 42.3–0.1	na	na	1650				
IRC–30363	0.241±0.130	54	720				
IRC+10322	0.553±0.183	33	570				
IRC+10451	0.818±0.196	24	730				
OH 26.2–0.6	na	na	1330				
OH 51.8–0.1	na	na	1270				
OH 358.16+0.49	na	na	1507				
V1018 Sco	na	na	na				

†: Duration of our VLBI observations using VERA.

2008). Then, relative position of the target maser spots can be determined with respect to the position reference source with an accuracy of less than 0.1 mas. By tracking the skyplane motions of the maser spots, we derive annual parallax of the target.

The signals of left-handed circular polarization from the target and position reference source were acquired with a total data recording rate of 1 giga-bit per second (Gsps). It gives a total bandwidth of 256 MHz. The data were recorded onto the hard disks of the “OCTADISK” system (Oyama *et al.* 2016). This entire bandwidth is divided into 16 IF channels. Each IF channel then has a width of 16 MHz. Then one IF channel (16 MHz) was assigned for the maser source and the remaining 15 IF channels (16 MHz × 16 = 240 MHz) were assigned to the position reference sources. Correlation processing was done with the Mizusawa software correlator at Mizusawa VLBI observatory, NAOJ. In the final output from the correlator, the 16 MHz bandwidth data of H<sub>2</sub>O or SiO masers was divided into 512 channels with a frequency resolution of 31.25 kHz. This corresponds to a velocity resolution of 0.42 km s<sup>–1</sup> at 22 GHz and 0.21 km s<sup>–1</sup> at 43 GHz.

### 2.3. Target sources

From 2017, we started observations of OH/IR stars in addition to Mira variables. In Table 1, we show target sources of our study. For the sources in the left part of the table, astrometric VLBI observations were made between 2017 and 2022. Although successful observations of all the sources were difficult, data acquisition for some stars has been completed and data reduction is currently underway. In 2023, we proposed VLBI observations of the new sources presented in the right part of the table. Parallaxes from the Gaia DR3 ( $\Pi_{\text{DR3}}$ ) and its relative errors are also presented. For the sources for which no parallax values were found in the Gaia DR3, we indicated “na” in the columns of  $\Pi_{\text{DR3}}$  and Err. In some sources, parallaxes show negative values. In addition, several other sources have errors larger than 100 %. As a result, the table shows that it is very difficult for Gaia to determine the accurate parallax of OH/IR stars. Therefore, the VLBI method is still important in parallax measurements of these dust-obscured OH/IR stars. We can also find various pulsation periods in the table. For the sources at low galactic latitudes and indicating longer period, we can expect that they are young and more massive than typical Mira variables.

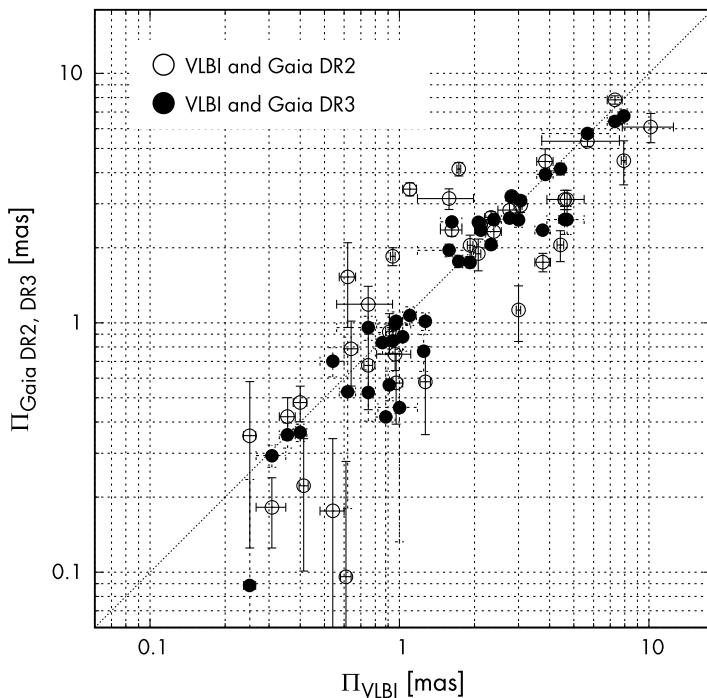


**Figure 1.** Annual parallaxes determined from VLBI (horizontal axis) and Gaia (vertical axis) in logarithmic scale. Open circles correspond to the comparison between VLBI and Gaia DR2, filled circles correspond to the comparison between VLBI and Gaia DR3.

### 3. Results and discussion

#### 3.1. Comparison between VLBI and Gaia

In Figure 1, we present parallaxes of AGB stars determined from VLBI ( $\Pi_{\text{VLBI}}$ ) and Gaia DR2/DR3 ( $\Pi_{\text{Gaia DR2}}$ ,  $\Pi_{\text{Gaia DR3}}$ ). Horizontal and vertical axes represent parallax values in logarithmic scales. Open (filled) circles represent comparison between VLBI and Gaia DR2 (Gaia DR3). A dotted line shows a relation of  $\Pi_{\text{VLBI}} = \Pi_{\text{Gaia}}$ . The dispersion of the filled circles is clearly smaller than that of open circles, which indicates that in many sources the two parallax measurements are closer to the same value in VLBI and Gaia DR3. However, we can find that there is still a large difference for a filled circle at the VLBI parallax of 0.247 mas (a filled circle at the bottom). We know that this data point corresponds to an OH/IR star NSV17351. Although we are curious about other OH/IR stars as well, they could not be presented on this figure because Gaia parallaxes of many dust-obscured OH/IR stars are not available.

#### 3.2. Results of individual sources

##### 3.2.1. NSV17351 (OH/IR star)

We determined pulsation period of NSV17351 from our single dish monitoring of H<sub>2</sub>O maser at 22GHz. From our least-squares analysis assuming a simple sinusoidal function, the pulsation period of NSV17351 was solved to be  $1122 \pm 24$  days (Nakagawa *et al.* 2023). The model fitting is presented with a solid curve in the left panel of Figure 2. As we cannot find any information on the period in the literature or online databases, this

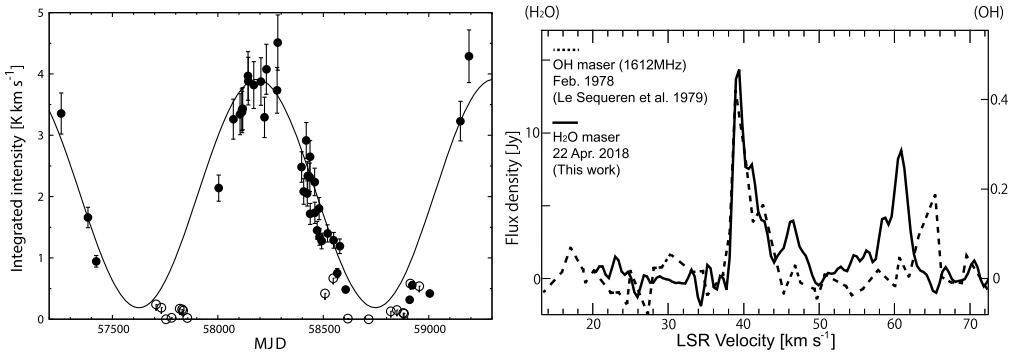


**Figure 2.** (Left): Time variation of the integrated H<sub>2</sub>O maser intensities of NSV17351. Filled circles represent results of successful detection. In the case of non-detection, we put open circles with downward arrows as representatives of detection upper limits. Solid line is the model indicating a pulsation period of  $1122 \pm 24$  days. (Right): Superpositions of H<sub>2</sub>O maser (solid line) and OH maser (dotted line) of NSV17351 obtained in 2018 and 1978, respectively. Cut off velocity of the blue-shifted side seems to be exactly same in both spectra.

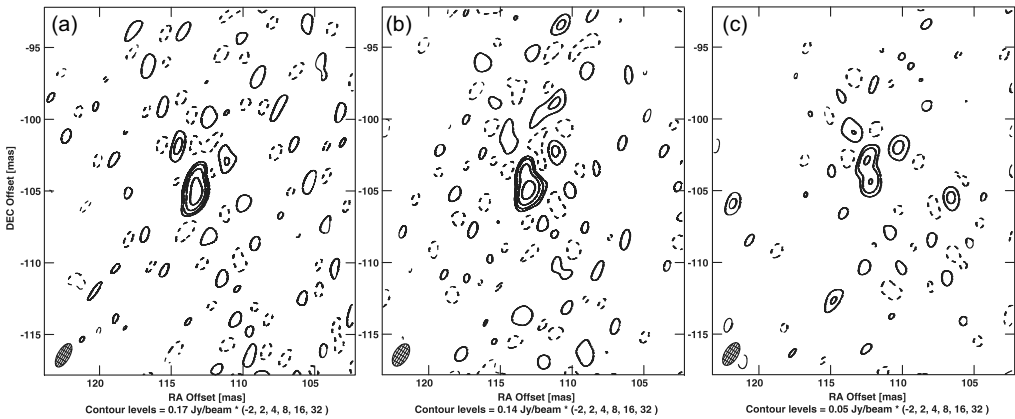


**Figure 3.** VLBI images of maser spots of NSV17351 at  $V_{\text{LSR}}$  of  $39.15 \text{ km s}^{-1}$  detected on (a) 16 April 2018, (b) 1 November 2018 and (c) 12 March 2019 (Nakagawa *et al.* 2023). The synthesized beams are presented at bottom left of each map.

is the first time we have measured the periodicity. We think NSV17351 is a candidate of extreme OH/IR stars because of its long periodicity.

In the right panel of Figure 2, we superposed H<sub>2</sub>O maser spectrum on 22 April 2018 (solid line) and 1612 MHz OH maser spectra in February 1978 (dotted line). We can find that the cut off velocity in the blue-shifted component shows exactly same velocity ( $38 \text{ km s}^{-1}$  to  $40 \text{ km s}^{-1}$ ). Since it is thought that OH molecules are supplied by photodissociation of H<sub>2</sub>O molecules carried to the outer part of the circumstellar envelope, we comprehend that the H<sub>2</sub>O molecules were carried to the outermost region and the H<sub>2</sub>O gas has accelerated to the terminal velocity.

Using VERA observation of H<sub>2</sub>O maser at 22GHz from 2018 to 2019, we derived a parallax of  $0.247 \pm 0.035 \text{ mas}$ , which corresponds to a distance of  $4.05 \pm 0.59 \text{ kpc}$ . In Figure 3, examples of maser spot images at the same velocity channel are presented. As the shape of the spot gradually changes with time, we carefully examined the maser structure, its time variation and continuity, then we concluded that the southern components in the

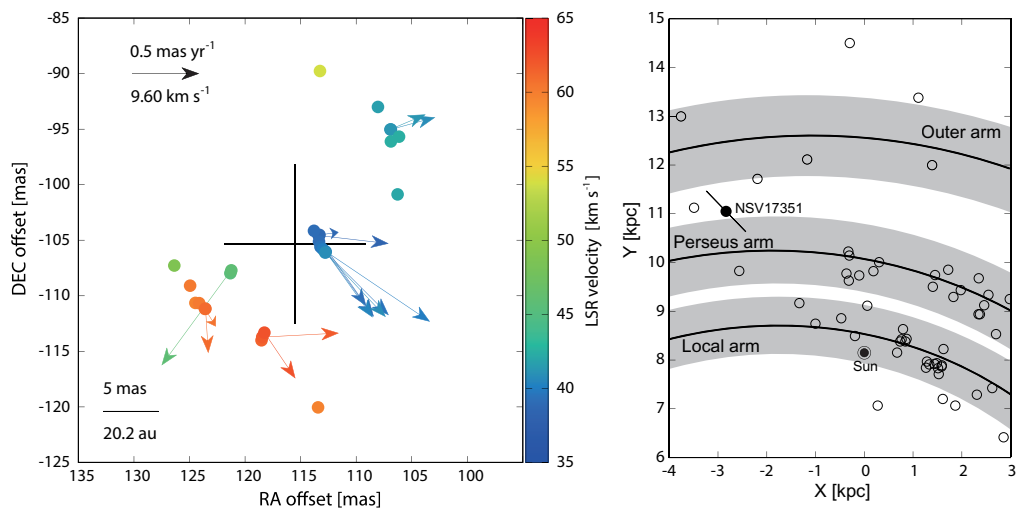


**Figure 4.** (Left): Skyplane distribution and expanding motions of H<sub>2</sub>O maser spots of NSV17351 Nakagawa *et al.* (2023). Filled circles indicate maser spots and arrows indicate their internal motions. A cross symbol indicates an estimated position of the central star. (Right): Location of NSV17351 on the face-on view of the Milky Way. The Galactic center is at (0, 0) kpc and the Sun is indicated with the symbol (⊙) at (0, 8.15) kpc. The filled circle with an error bar indicates the position of NSV17351. Open circles indicate maser sources which have Galactocentric distances of > 7 kpc. Solid lines and grey regions indicate centers of three spiral arms and their widths reproduced from a study by Reid *et al.* (2019).

maps (b) and (c) are identical to the peak in map (a). Stellar system proper motion of  $(\mu_{\alpha} \cos \delta, \mu_{\delta}) = (-1.19 \pm 0.11, 1.30 \pm 0.19) \text{ mas yr}^{-1}$  was also obtained. Circumstellar distribution and motions of H<sub>2</sub>O masers in  $80 \times 120 \text{ au}$  area is presented in the left panel of Figure 4. We derived an outward expansion velocity of the H<sub>2</sub>O masers to be  $15.7 \pm 3.3 \text{ km s}^{-1}$ . Estimated stellar positions are indicated by cross symbols, the lengths of which represent the position errors. Bluest maser spots overlap estimated position of central star.

In the right panel of Figure 4, we can find that NSV17351 is located slightly outside the Perseus arm. The location of NSV17351 can be understood by considering the age. Feast (2009) reported that Mira variables showing a period of 1000 d have initial masses of 3 to  $4 M_{\odot}$ . By assuming this mass, we can estimate age of NSV17351 to be  $1.6 \times 10^8$  to  $3.5 \times 10^8$  years. The age of NSV17351 is two orders of magnitude larger than the typical age of high mass star forming regions associated with spiral arms, and we can say that we are observing a state that NSV17351 leaves the arm where it was born, but not yet sufficiently dynamically relaxed.

### 3.2.2. OH39.7+1.5, IRC-30363 (OH/IR star) and AW Tau (Mira)

We observed H<sub>2</sub>O masers in OH39.7+1.5, IRC-30363 (OH/IR star), and AW Tau (Mira) at 22GHz. For OH39.7+1.5, using two maser spots at radial velocities of 34.6 and  $8.6 \text{ km s}^{-1}$ , a parallax of  $0.54 \pm 0.03 \text{ mas}$  was obtained. This corresponds to a distance of  $1.85 \pm 0.10 \text{ kpc}$ . Averaged proper motion of the two maser spots is  $(\mu_x, \mu_y) = (-0.22 \pm 0.13, -1.53 \pm 0.13) \text{ mas yr}^{-1}$ . For IRC-30363, using a maser spots at radial velocities of  $9.72 \text{ km s}^{-1}$ , a parallax of  $0.562 \pm 0.201 \text{ mas}$  was obtained. This corresponds to a distance of  $1.78 \pm 0.73 \text{ kpc}$ . For AW Tau, using a maser spots at radial velocities of  $-9.54 \text{ km s}^{-1}$ , a parallax of  $0.449 \pm 0.032 \text{ mas}$  was obtained. This corresponds to a distance of  $2.23 \pm 0.16$

kpc. Pulsation periods of OH39.7+1.5, IRC–30363 (OH/IR star) and AW Tau are 1260, 720, and 672 days, respectively. All sources shows longer pulsation periods than typical Mira variables.

### 3.3. Absolute magnitude in near-IR and mid-IR

We estimated absolute K-band magnitudes (M<sub>k</sub>) of three AGB stars, AW Tau, IRC–30363, and OH39.7+1.5 based on parallax measurements in the previous section. When we compare the three M<sub>k</sub> values with a period-M<sub>k</sub> diagram of the Galactic long period variables, we found that M<sub>k</sub> of OH39.7+1.5 is far below the expected value. If we assume thick dust layer or high mass loss rate for the OH/IR star OH39.7+1.5, we can possibly explain this darkening due to circumstellar absorption.

We also estimated absolute magnitudes of the three sources in mid-infrared using WISE W3 band. The central wavelength of the W3 band is 12 μm (Wright *et al.* 2010). The absolute magnitudes M<sub>W3</sub> of AW Tau, IRC–30363, and OH39.7+1.5 were obtained to be  $-10.71 \pm 0.16$ ,  $-12.35 \pm 0.81$ , and  $-12.94 \pm 0.12$ , respectively. When considered in conjunction with our preliminary results obtained so far, absolute magnitudes M<sub>W3</sub> of various AGB stars seems to represent a unified relation along pulsation period in mid-infrared. To confirm the indication of the period-M<sub>W3</sub> relation, we have to continue astrometric VLBI observations of OH/IR stars with wide period range.

## 4. Summary

We are observing Miras and OH/IR stars with astrometric VLBI. Acquired distances and stellar parameters helps us to understand evolutionary relation of sub-classes in AGB phase. The VERA was used to conduct all the VLBI observations of H<sub>2</sub>O (22 GHz) and SiO (43 GHz) masers. Phase referencing technique was used to measure parallaxes. Results of NSV17351, AW Tau, IRC–30363, and OH39.7+1.5 were presented here. Absolute magnitudes in near-infrared and mid-infrared bands were derived based on the obtained parallaxes. Indication of a new period-magnitude relation in mid-infrared (WISE W3 band) band can be found. For further understanding, we need more detailed measurements of the circumstellar masers of AGB stars with various types, pulsation periods, and masses.

## References

- Chiavassa, A., Freytag, B., & Schultheis, M. 2018, *A&A*, 617, L1  
 Cox, J. P. 1980, *Theory of Stellar Pulsation. (PSA-2)*, Volume 2. John P. Cox. ISBN: 9781400885855. Princeton University Press, 1980  
 Feast, M. W. 2009, *AGB Stars and Related Phenomena*, 48  
 Gaia Collaboration, Vallenari, A., Brown, A. G. A., *et al.* 2022, arXiv:2208.00211  
 Honma, M., Kijima, M., Suda, H., *et al.* 2008, *PASJ*, 60, 935  
 Justtanont, K., Barlow, M. J., Blommaert, J., *et al.* 2015, *A&A*, 578, A115  
 Kamizuka, T., Nakada, Y., Yanagisawa, K., *et al.* 2020, *ApJ*, 897, 42  
 Karakas, A. I. & Lattanzio, J. C. 2014, *PASA*, 31, e030  
 Karambelkar, V. R., Adams, S. M., Whitelock, P. A., *et al.* 2019, *ApJ*, 877, 110  
 Kawaguchi, N., Sasao, T., & Manabe, S. 2000, *Proc.SPIE*, 4015, 544  
 te Lintel Hekkert, P., Caswell, J. L., Habing, H. J., *et al.* 1991, *A&AS*, 90, 327  
 Matsuno, M., Nakagawa, A., Morita, A., *et al.* 2020, *PASJ*, 72, 56  
 Nakagawa, A., Kurayama, T., Matsui, M., *et al.* 2016, *PASJ*, 68, 78  
 Nakagawa, A., Kurayama, T., Orosz, G., *et al.* 2018, *Astrophysical Masers: Unlocking the Mysteries of the Universe*, 336, 365  
 Nakagawa, A., Morita, A., Sakai, N., *et al.* 2023, *PASJ*, 75, 529



- Nyu, D., Nakagawa, A., Matsui, M., *et al.* 2011, *PASJ*, 63, 63  
Oyama, T., Kono, Y., Suzuki, S., *et al.* 2016, *PASJ*, 68, 105  
Reid, M. J., Menten, K. M., Brunthaler, A., *et al.* 2019, *ApJ*, 885, 131  
Takeuti, M., Nakagawa, A., Kurayama, T., *et al.* 2013, *PASJ*, 65, 60  
Wright, E. L., Eisenhardt, P. R. M., Mainzer, A. K., *et al.* 2010, *AJ*, 140, 1868